Characterization and Application of Nanomaterials (2022) Volume 5 Issue 2
doi:10.24294/can.v5i2.1768

ORIGINAL RESEARCH ARTICLE

Development, optimization, and evaluation of Cisplatin-loaded PLGA nanoparticles

Purushothaman Bhuvaneshwaran, Ramaiyan Velmurugan*

Faculty of Pharmaceutical Sciences, Saveetha Institute of Medical and Technical Sciences, Chennai, Tamil Nadu 602105, India. E-mail: ramaiyan.dr@gmail.com

ABSTRACT

Nanoparticle drug delivery systems are engineered technologies that use nanoparticles for the targeted delivery and controlled release of therapeutic agents. Cisplatin-loaded nanoparticle formulations were optimized utilizing response surface methods and the central composite rotating design model. This study employed a central composite rotatable design with a three-factored factorial design with three tiers. Three independent variables namely drug polymer ratio, aqueous organic phase ration, and stabilizer concentration were used to examine the particle size, entrapment efficiency, and drug loading of cisplatin PLGA nanoparticles as responses. The results revealed that this response surface approach might be able to be used to find the best formulation for the cisplatin PLGA nanoparticles. A polymer ratio of 1:8.27, organic phase ratio of 1:6, and stabilizer concentration of 0.15 were found to be optimum for cisplatin PLGA nanoparticles. Nanoparticles made under the optimal conditions found yielded a 112 nm particle size and a 95.4 percent entrapment efficiency, as well as a drug loading of 9 percent. The cisplatin PLGA nanoparticles tailored for scanning electon microscopy displayed a spherical form. A series of in vitro tests showed that the nanoparticle delivered cisplatin progressively over time. According to this work, the Response Surface Methodology (RSM) employing the central composite rotatable design may be successfully used to simulate cisplatin-PLGA nanoparticles.

Keywords: Cisplatin; PLGA; Nanoparticles; Response Surface Methodology; Central Composite Rotatable Design

ARTICLE INFO

Received: 2 August 2022
Accepted: 28 September 2022
Available online: 12 October 2022

1. Introduction

Tumors form when cells grow and divide improperly and uncontrollably, which is the hallmark of the cancerous condition. New technologies that can distinguish between healthy and cancerous cells followed by the targeting of the tumor with precision are attracting a lot of attention. With (Transdermal drug delivery) TDD, the medicine is encapsulated inside of a nanocarrier like liposomes or liposomal particles to transport it directly to the patient. Both the effectiveness and toxicity of the medicine may be improved by TDD, and it can overcome a broad variety of difficulties, such as drug solubility and instability, and the ease of delivery to the target cells. Passive and active medication targeting methods are available[1]. On the basis of the enhanced permeability and retention (EPR) effect, which occurs in most solid tumors, passive targeting relies on molecules of specific sizes being preferentially taken up and retained by the tumors[2]. However, the reticuloendothelial system (RES) rapidly removes intravenously delivered nanocarriers containing anticancer medicines from circulation. These nanocarriers have a hydrophilic polymer, for example, polyethylene glycol (PEG) coating applied on top of them to increase their circulation duration and consequently

their targeting of tumor tissue[3]. The adsorption of plasma proteins (opsonin), which is critical for phagocytosis, would be prevented, resulting in a longer period for blood to circulate[4,5]. Nanoparticles (NPs) are regarded as drug delivery mechanism that allows for novel approaches to cancer therapy, and one of the most important methods used in nanomedicine. There are several NP delivery techniques, in which the medication is dissolved, encapsulated, and entrapped inside the matrix[6]. The potential of NPs coupled with biodegradable polymers such as PLGA to actively and passively target tumors has drawn considerable interest[7]. The exterior diameters of NPs can range from a few nanometers to over 1,000 nanometers in length. Due to the EPR effect, NPs coated with PEG can accumulate in a variety of solid tumors, making them ideal carriers for hydrophobic medicines, which can provide effective tumor targeting with the fewest adverse responses[8,9]. Nanoprecipitation[10], solvent evaporation[11], dialysis[12], and salting out[13] have all been used for the formation of NPs.

For the treatment of a wide range of solid malignancies, including cervical cancer, cisplatin is a powerful anticancer drug[14]. In order to eliminate cancer cells, cisplatin causes cross-linking of DNA, which leads to cell death.

Although cisplatin has a powerful anticancer impact, its severe side effects such as nephrological and neurological toxicities[15] limit its effectiveness. Chronic and acute kidney damage are common side effects of cisplatin, while neurotoxicity is cumulative-dose dependent. Cisplatin's immediate inactivation in the systemic circulation is one of the greatest concerns[16,17]. As a result, cis-dichlorodiammineplatinum (II) (cis-[PtCl2(NH3)2], cisplatin (CDDP's) pharmacological effect must be protected and its systemic circulation must be prolonged. Drug must be delivered over an extended period of time in order to maximise its anticancer properties and minimise its negative effects.

For passive targeting following intravenous delivery, researchers are trying to integrate cisplatin into poly (lactic-coglycolic acid) (PLGA) NPs. Response Surface Methodology - Central Composite Rotatable Design will be used to optimise the nanoparticles created. After optimizing cisplatin loading, we will conduct *in vitro* drug release and physicochemical evaluations of the PLGA NPs.

2. Materials and method

Dichloromethane and sodium cholate were provided by Madras pharmaceuticals, India. Cisplatin and PLGA was purchased from Sigma-Aldrich, India. All other chemicals were of analytical grade and used as such.

2.1 Preparation of cisplatin nanoparticles

In order to create nanoparticles, a solvent evaporation approach was used[18]. Sonication was used for 5 min to create an emulsion between an organic polymer solution (o) and an aqueous solution (w) containing the medication (5 mg of cisplatin in 2 mL distilled water). It was then mixed with 50 mL of water and sonicated to create the double-emulsion, which was then dissolved in an equal amount of water. A mild magnetic stirring at room temperature was used to evaporate the solvent. Recovered nanoparticles were rinsed with distilled water, dried, and kept in cold temperatures (2–8 °C) for future use.

2.2 Experimental design

According to preliminary investigations, the variables including drug polymer ratio, water to organic phase ratio, and stabilizer concentration during synthesis of the cisplatin nanoparticles, had the greatest impact on particle size, distribution, entrapment, and drug loading efficiency. These responses were considered for optimization as they accounts very much for rapid drug absorption and drug availability. In order to study the impact of these three essential formulation factors on particle size, entrapment efficiency, and drug loading efficiency, a central composite rotatable design–response surface methodology (CCRD–RSM) was adopted[19]. **Table 1** lists the design specifications. Preliminary tests and the possibility of making nanoparticles at extreme levels were used to select the experimental ranges for each component. For the drug polymer ratio (X1), the range was 1:1–1:7; for the aqueous-to-organic phase ratio (X2), it was 1:1–1:5, and for the stabilizer concentration (X3), it was 0.1–0.5%. There were a

total of 20 tests carried out. In these tests, every formulation was made in two separate batches. Since it may investigate many variables at multiple levels with a small number of tests, the central composite rotating design–response surface methodology (CCRD–RSM) is an excellent alternative strategy. After conducting exploratory trials, we came up with the factors in **Table 1**. Particle size distribution, drug loading, and entrapment efficiency were all examined in **Table 2** of the experiments. 94–104 nm, 75–94 %, and 4–13% were the three dependent variables. Design-Expert® 7.0 software was used to perform response surface regression analysis on variables and parameters.

Table 1. Independent variables and their corresponding levels of Nanoparticle preparation for CCRD

Independent variables	**Levels**		
	−1	**0**	**+1**
Drug/polymer ratio	1:1	1:5	1:9
Aqueous to organic phase ratio	1:1	1:3.5	1:6
Stabilizer concentration	0.1	0.55	1.0

Table 2. Central composite design consisting of experiments for the study of three experimental factors in coded and actual levels with experimental results

S. NO	**Trial**	**Drug polymer ratio**	**Aqueous organic phase ratio**	**Conc. of stabilizer**	**Particle size**	**Entrapment efficiency**	**Drug loading**
1	1	1	1	0.1	100.335	84.076	7.231
2	2	9	1	0.1	99.3895	83.012	8.254
3	3	1	6	0.1	96.8928	81.123	9.014
4	4	9	6	0.1	96.3544	79.089	8.543
5	5	1	1	1	97.9656	87.12	11.239
6	6	9	1	1	95.3729	75.13	13.231
7	7	1	6	1	103.267	85.065	10.123
8	8	9	6	1	102.642	89.87	11.435
9	9	−1.72717	3.5	0.55	102.176	92.1009	5.098
10	10	11.7272	3.5	0.55	104.079	79.34	11.675
11	11	5	−0.704482	0.55	102.726	84.012	9.233
12	12	5	7.70448	0.55	94.2578	90.012	5.987
13	13	5	3.5	−0.206807	96.3522	89.122	9.234
14	14	5	3.5	1.30681	104.532	93.9741	5.123
15	15	5	3.5	0.55	98.5098	91.012	4.098

2.2.1 Particle size analysis

A Malvern Zetasizer 3000 HSA was used to measure particle size using dynamic light scattering (DLS) (Malvern Instruments, UK). The polydispersity index (PI), a measure of the breadth of the size distribution, and the mean diameter are both obtained using DLS. Temperatures of 25 °C were used to measure the mean diameter and the proportional index (PI). An acceptable scattering intensity was achieved by diluting all samples with double-distilled water prior to testing.

2.2.2 Zeta potential

Zeta potential, which reflects the electric charge on a particle's surface and indicates its physical stability, was determined by measuring electrophoretic mobility using the Malvern Zetasizer 3000 HSA (**Figure 9**) (Malvern Instruments, UK). Sodium chloride solution (0.9% w/v) was used to modify the conductivity of the sample to 50 IS/cm in double distilled water. The applied field strength was 20 V/cm and the pH ranged between 5.5 and 7.5.

2.2.3 Scanning Electron Microscopy (SEM) measurement

Using a Hitachi S4800 Field Emission Scanning Electron Microscope (FESEM), the surface and surface morphology of the particles were analyzed in detail (Hitachi, Gaithersburg,

MD, USA). Analysis settings comprised a vacuum pressure of 40 Pascals, an accelerating voltage of 10 keV, and a working distance of 13.5 mm

2.2.4 Differential Scanning Calorimetry (DSC) analysis

Pure cisplatin, PLGA, physical mixtures, and cisplatin nanoparticles were all examined using a differential scanning calorimeter (DSC) (Shimadzu DSC-60, Columbia, MD, USA). It was crimped non-hermetically in an aluminum pan and heated at a rate of 10 °C/min from 23 °C to 300 °C under a nitrogen purge for DSC analysis (3–5 mg).

2.2.5 Fourier Transform Infrared spectroscopy (FTIR) analysis

FTIR analyses of cisplatin, PLGA, physical mixture and cisplatin nanoparticles were carried out using IR Prestige-21 (Shimadzu, Columbia, MD, USA). The sample was placed in direct contact with ATR crystal ensuring good contact. All the spectra were recorded as a mean of 20 scans, with a resolution of 4 cm^{-1} and in the range of 800 to 4,000 cm^{-1}.

2.2.6 Chromatographic conditions

Chromolith RP-18e (E-Merk, 4.6 × 50 mm) column was used to measure the cisplatin concentration in the HPLC system[20]. An acetonitrile-water mixture containing 0.1% formic acid (40:60) was utilized as the mobile phase. A flow rate of 0.5 mL/min was measured. 10 µL of injection was used with a 490 nm laser and a wavelength of 10 nm.

2.2.7 Determination of drug entrapment efficiency (EE) and drug loading (DL)

Centrifuged nanoformulations were evaluated by HPLC[21], and the supernatant containing the free drug, which was recovered, was further studied. Unentrapped nanoparticles of drug may be determined using this method. In order to determine the amount of drug encapsulated in nanoparticles, a subtraction was made from the total amount of drug added to the formulation. For the evaluation of the formulations, the following formula was used:

$$EE = \frac{Amount\ of\ drug\ in\ nanopartilce}{Amount\ of\ drug - Loaded\ nanoparticle} \times 100$$

$$DL = \frac{Amount\ of\ drug\ in\ \ nanoparticle}{Amount\ of\ drug\ for\ loading} \times 100$$

2.2.8 *In vitro* release study

Dialysis bags (cellulose membrane, 12400MW, Sigma) were used to contain nanoparticle samples, which were incubated in 30 mL of PBS (pH 7.4) at 37 °C under gentle agitation in a water bath at 37 °C (20). Samples were taken from the incubation mixture at predefined intervals and tested for cisplatin using the HPLC technique as described above. Every time a sample was taken, the incubation media was changed with new PBS. In addition, a control experiment was conducted to assess the free drug's release behavior. Dialysis bags were filled with PBS, PBS at 37 °C, and dissolved cisplatin in 1 mL of this solution, which was deposited in 30 mL of PBS. It was determined that cisplatin was released in the manner stated above.

2.3 Data analysis

Design-Expert® software was used to analyze the connections between model responses and their corresponding formulation factors. Stepwise linear regression and response surface analysis were used in the statistical study. In the final equations, only significant terms ($p < 0.05$) were used. Linear, quadratic, and special cubic models are all suitable for three-component models. On the basis of statistical comparisons of a number of statistical parameters, including the coefficient of variation (CV), the multiple correlation coefficient (R^2), and an adjusted multiple correlation coefficient (adjusted R^2) proved by Design-Expert software, the best fitting mathematical model was selected. Student's t-test and one-way ANOVA were used to determine the significance of differences at a 0.05 significance level.

3. Results and discussion

3.1 Optimization of formulas

According to the most statistically significant factors on the examined parameters, 3D response surface graphs are provided in **Figures 1–3**. The experiment yielded a desirability of 0.542 (**Figure 4**). Particle size and entrapment efficiency improve with a rise in polymer content and the aqueous to organic phase ratio. Polymer concentration and aqueous to organic phase ratio both reduce drug loading. The correlation coefficients (*r*) of the optimized variables were 0.9365, 0.9289, and 0.9698, respectively, for the second-order polynomial equation. The *r* value reduced significantly to 0.9112, 0.2089, and 0.9312 after model simplification with backward stepwise solution. At a 95% confidence level, there was a substantial lack of fit. At $p <$ 0.05, all of the remaining variables were significant. The best-fitting model was the quadratic model, and the comparative values of R, SD, and percent CV along with the regression equation developed for the selected answers are shown in **Table 3**. The following polynomial equations were derived from the statistical analysis of the results:

$$PS = +98.57 - 0.1099A - 0.5967B + 1.47C + 0.2968AB - 0.2167AC + 2.38BC + 1.25A^2 - 0.3845B^2 + 0.3050C^2$$

$$EE = +91.17 - 2.32A + 1.16B + 1.32C + 1.98AB - 0.5109AC + 2.45BC - 2.90A^2 - 2{,}44B^2 - 0.8352C^2$$

$$DL = +4.04 + 1.09A - 0.4612B + 0.4446C - 0.2717AB + 0.3440AC - 0.6230BC + 1.93A^2 + 1.65B^2 + 1.50C^2$$

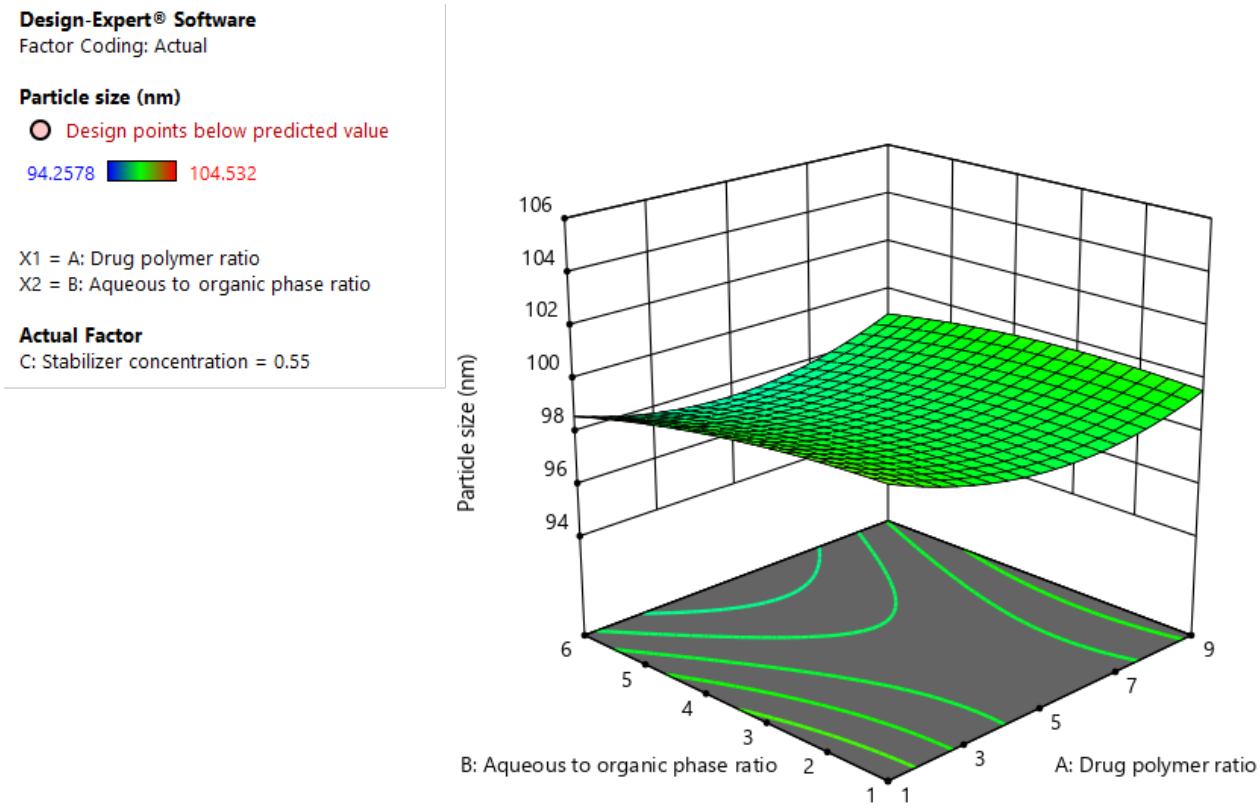

Figure 1. Three-dimensional (3D) response surface plots showing the effect of drug/polymer ratio and aqueous to organic phase ratio on particle size.

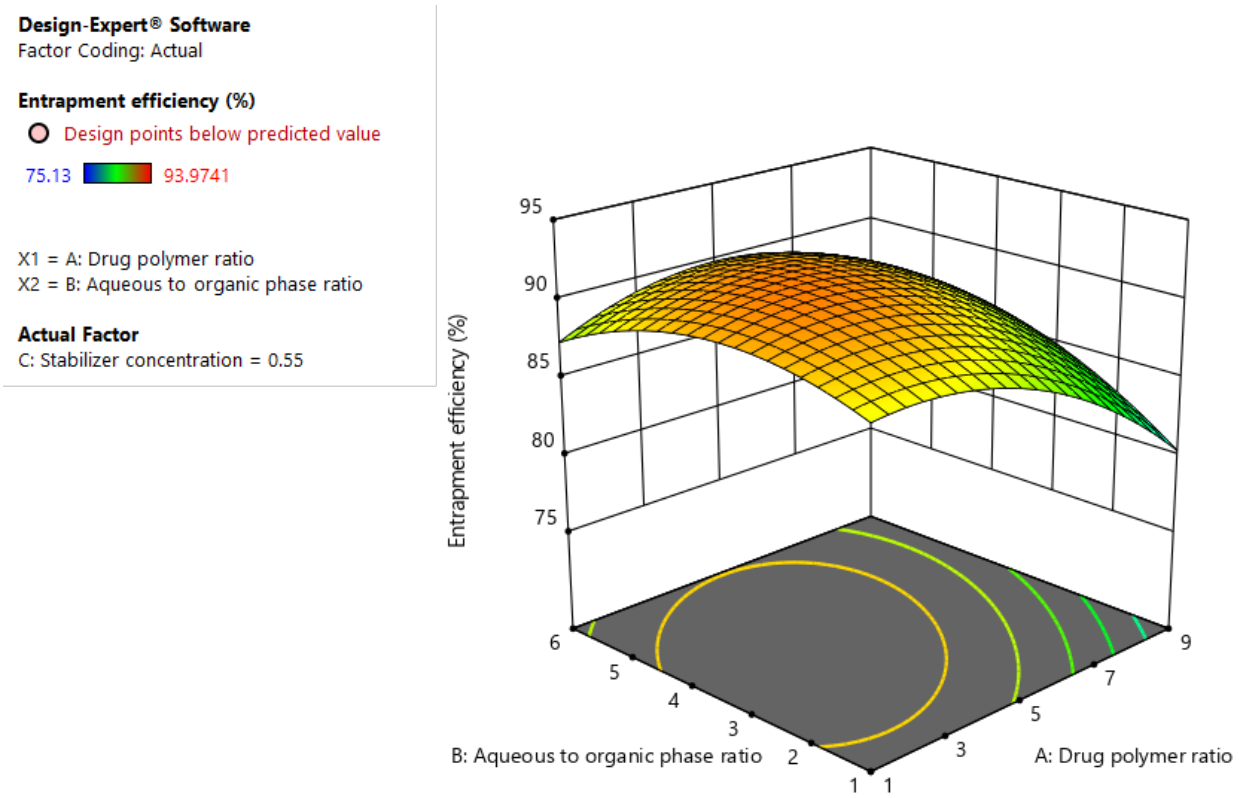

Figure 2. Three-dimensional (3D) response surface plots showing the effect of drug/polymer ratio and aqueous to organic phase ratio on entrapment efficiency.

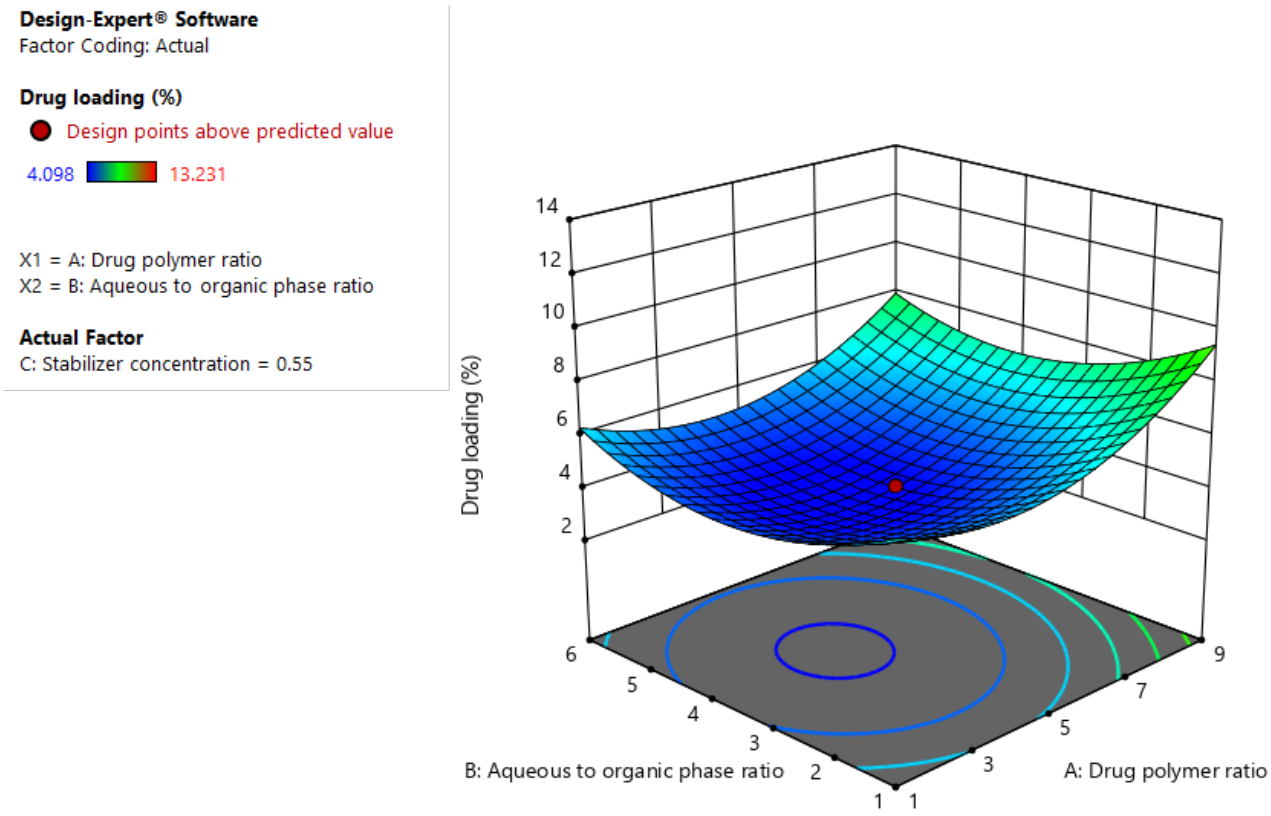

Figure 3. Three-dimensional (3D) response surface plots showing the effect of drug/polymer ratio and aqueous to organic phase ratio on drug loading.

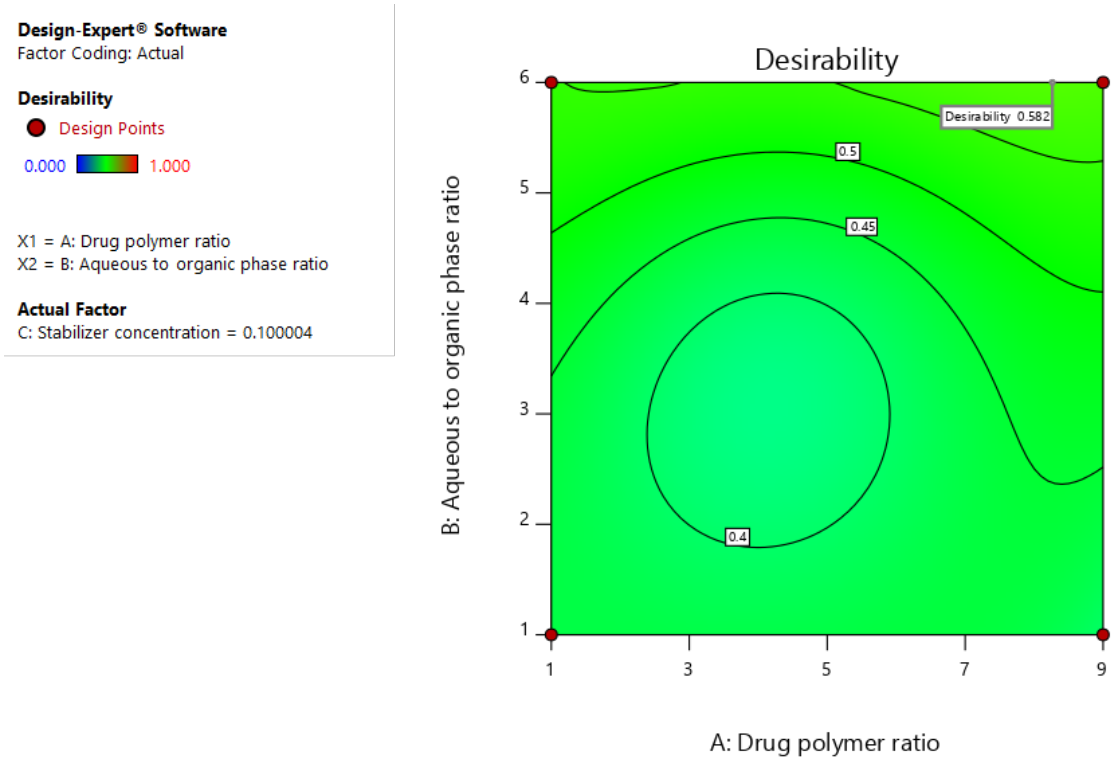

Figure 4. Contour plot showing the desirability with a value of 0.542.

Table 3. Reduced response models and statistical parameters obtained from ANOVA

Responses	Regression model	Adjusted R^2	Model *P* value	% CV	Adequate precision
Particle size	PS = +98.57 – 0.1099A – 0.5967B + 1.47C + 0.2968AB – 0.2167AC + 2.38BC + 1.25A^2 – 0.3845B^2 + 0.3050C^2	0.9365	0.0001	2.86	6.47
Entrapment efficiency	EE = +91.17 – 2.32A + 1.16B + 1.32C + 1.98AB – 0.5109AC + 2.45BC – 2.90A^2 – 2,44B^2 – 0.8352C^2	0.9289	0.0001	3.12	9.10
Drug loading	DL = +4.04 +1.09A – 0.4612B + 0.4446C – 0.2717 AB + 0.3440AC – 0.6230BC + 1.93A^2 + 1.65B^2 + 1.50C^2	0.9698	0.0001	3.98	11.28
Acceptance criteria		1	<0.05	<4	>4

A drug polymer to aqueous/organic phase ratio of 1:6 and a stabilizer concentration of 0.1% produced nanoparticles with high EE, high DL, and a small mean diameter, according to the fitting findings. Data from the two batches that were created in optimal ranges were extremely near to the projected values, with a minimal percentage bias. This indicates that the optimized formulation was trustworthy and reasonable. **Figures 5–7** show the effect of an independent factor on a specific response, with all other characteristics maintained constant at a reference factor. A high inclination or curve indicates that the reaction to a given element is very sensitive. The aqueous-to-organic phase ratio, drug polymer ratio, and stabilizer concentration are all shown to have significant effects on particle size in **Figure 5**. Following stabilizer concentration and drug polymer ratio, the aqueous to organic phase ratio had the most significant influence on entrapment efficiency, as shown in **Figure 6**. Drug polymer ratio, stabilizer concentration, and aqueous-to-organic phase ratio are shown in **Figure 7** to have the most significant effect on drug loading. Response surface methodology (RSM) using the central composite rotatable

design model was used to optimize formulations of dihydroartemisinin nanostructured lipid carrier. The experimental values of the nanoparticles prepared under the optimum conditions were mostly close to the predicted values (**Table 4**)[22]. The ansamycin-loaded polymeric nanoparticles were optimized using the central composite rotatable design–response surface methodology by fitting a second-order model to the response data and the experimental values of the nanoparticles shows that it deliver the encapsulated drug well to the target site[23].

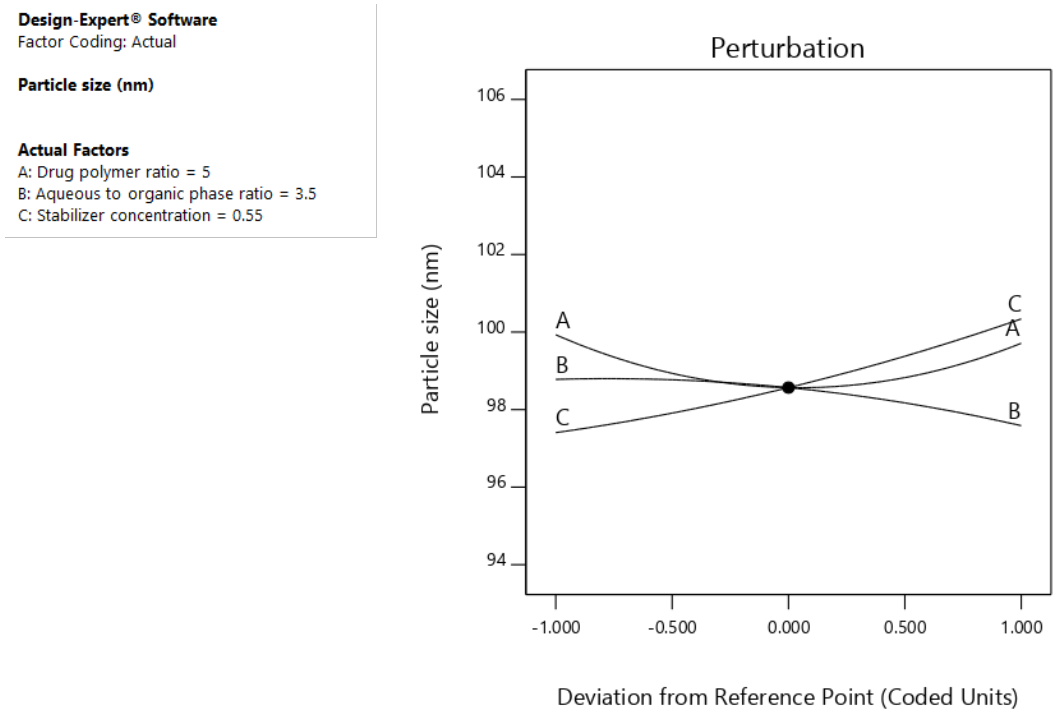

Figure 5. Perturbation plot showing the effect of independent variables on Particle size where A, B and C are Drug/polymer ratio, aqueous to organic phase ratio and stabilizer concentration respectively.

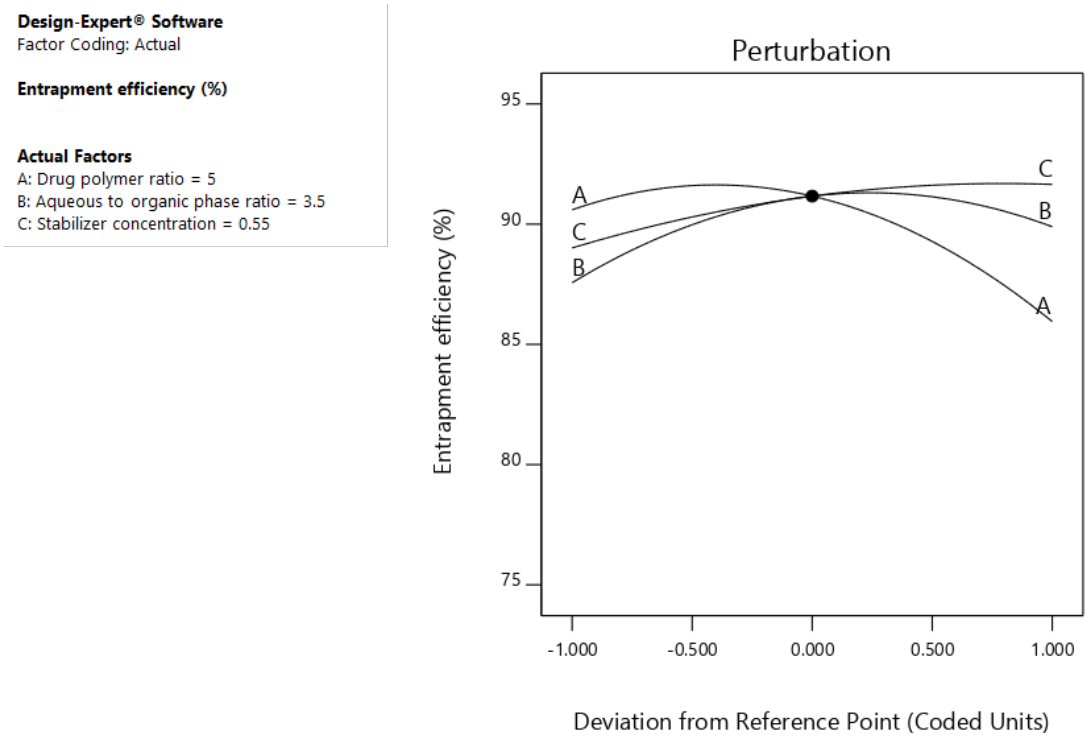

Figure 6. Perturbation plot showing the effect of independent variables on entrapment efficiency where A, B and C are Drug/polymer ratio, aqueous to organic phase ratio and stabilizer concentration respectively.

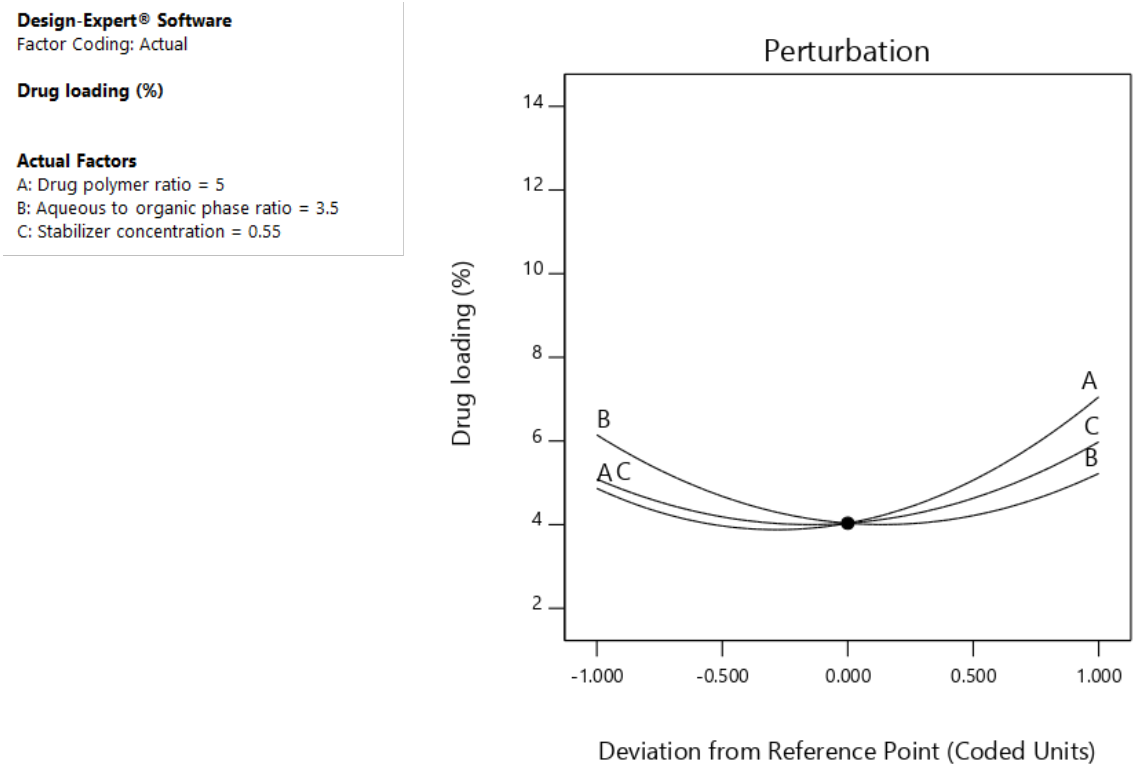

Figure 7. Perturbation plot showing the effect of independent variables on drug loading where A, B and C are Drug/polymer ratio, aqueous to organic phase ratio and stabilizer concentration respectively.

Table 4. Predicted and experimental values under predicted optimal conditions

Drug/polymer ratio	Aqueous to organic phase ratio	Stabilizer concentration (%)	Particle size (nm)	Entrapment efficiency (%)	Drug loading (%)
1:8.27	1:6	0.1			
Predicted			114	83.5	8.6
Experimental			112	85.4	9.0
Bias %			1.75%	2.27%	4.6%
Acceptance criteria 6%					
Bias was calculated as (predicted value - experimental value)/predicted value × 100					

3.2 Particle size, zeta potential and SEM measurement

It was discovered that the average cisplatin nanoparticle particle size was 112 nm (**Figure 8**). As shown in **Figure 9**, the zeta potential of this compound is high enough to allow for the creation of a stable pharmaceutical formulation. **Figure 10** shows the SEM images taken of the improved cisplatin nanoparticles to offer information on their shape. These nanoparticles have been fine-tuned to be spherical. The nanoparticles had the higher absolute values of zeta potential, indicating a better stability of this colloid system[24]. Zeta potential under −30 mV showed good physical stability[25].

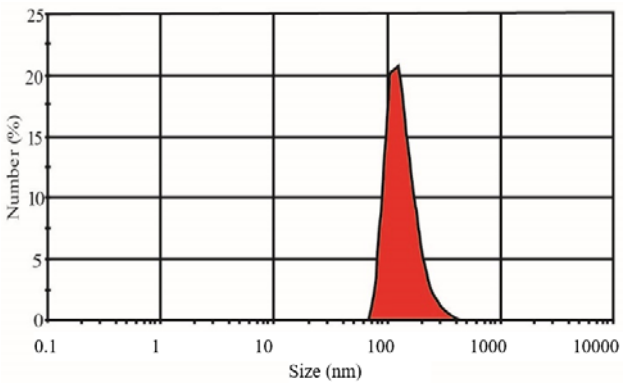

Figure 8. Size distribution of Cisplatin PLGA NP.

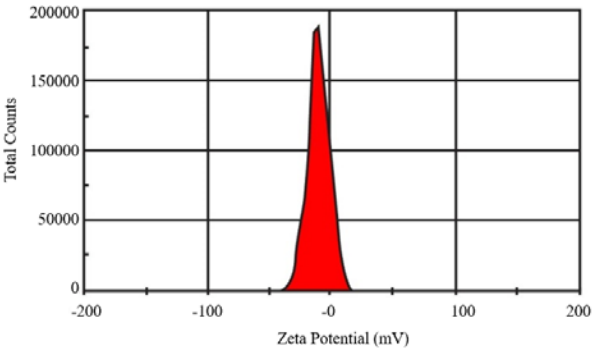

Figure 9. Zeta potential of Cisplatin PLGA NP.

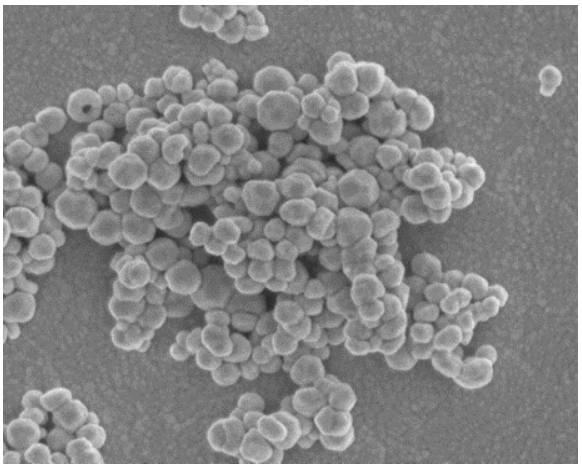

Figure 10. Scanning electron microscopy of Cisplatin PLGA NP.

3.3 Differential Scanning Calorimetry (DSC) analysis

After the preparation, DSC was used to examine the cisplatin's physical condition within the PLGA particles. Drug-loaded nanoparticles did not exhibit the glass transition peak seen in the DSC thermogram of PLGA (**Figure 11**). The cisplatin thermogram revealed an exothermic peak at 280–285 °C. It is possible that the drug is scattered in an amorphous form due to its lack of this characteristic peak.

3.4 Fourier Transform Infrared spectroscopy (FTIR) analysis

FTIR analysis is used to study the interactions between cisplatin and PLGA during the entrapment procedure and the FTIR spectrum obtained for cisplatin, PLGA, physical mixture and the drug loaded nanoparticle is presented in **Figure 12**.

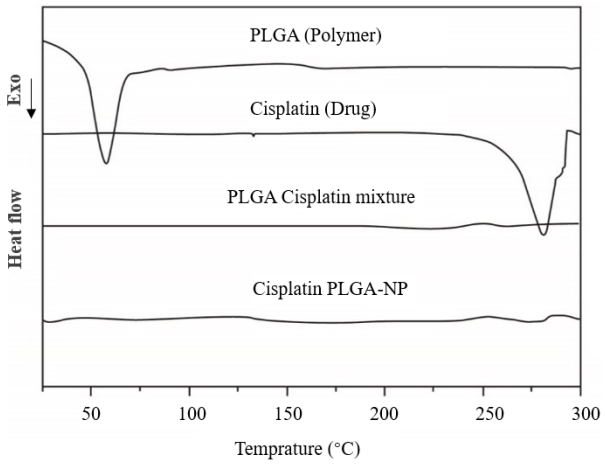

Figure 11. DSC thermogram of PLGA (polymer), Cisplatin (drug), PLGA Cisplatin mixture, Cisplatin PLGA NP.

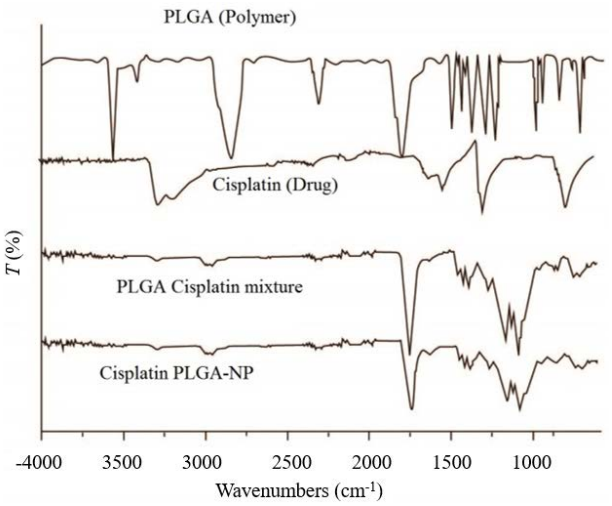

Figure 12. FTIR spectra of PLGA (polymer), Cisplatin (drug), PLGA Cisplatin mixture, Cisplatin PLGA NP.

The pure cisplatin obtained the characteristic peaks that includes amine stretching (3,208 cm^{-1}), symmetric amine bending (1,302 cm^{-1}) and chloride stretching (766 cm^{-1}). PLGA nanoparticles obtained its characteristic peaks that include C = O stretching (1,728 cm^{-1}) and C-O stretching (1,020–1,280 cm^{-1}). The FTIR spectra of the cisplatin loaded nanoparticles obtained a peak for amine stretching (3,279 cm^{-1}), indicating the presence of cisplatin in the formulation. The FTIR data obtained indicates that there were no chemical interactions between PLGA and the study drug cisplatin.

3.5 *In vitro* drug release study

In vitro cisplatin release from PLGA nanoparticles is presented in **Figure 13**. Biphasic

release pattern with an initial fast release for the first 48 hrs, followed by a steady release for six days is observed. The drug may have accumulated on the nanoparticle surface during manufacturing, resulting in a fast release. Comparison of cisplatin release profiles with those of cisplatin solution demonstrates that nanoparticle entrapment greatly slowed cisplatin's release from the solution. According to the data (**Figure 13**), roughly 90% of cisplatin in phosphate buffer solution was released in 24 hours. For the next six days, the cisplatin nanoparticles released at a consistent and modest rate. *In vitro*, the cisplatin nanoparticles showed a clear sustained-release impact as compared to cisplatin. The decreased percentage of cumulative drug release may be due to the enhanced particle size and also hence smaller sized surface area at greater polymer concentration. An additional description for reduced cumulative drug release at greater polymer concentration might be the enhanced concentration of the polymer existing which impedes the drug release by diffusion[26].

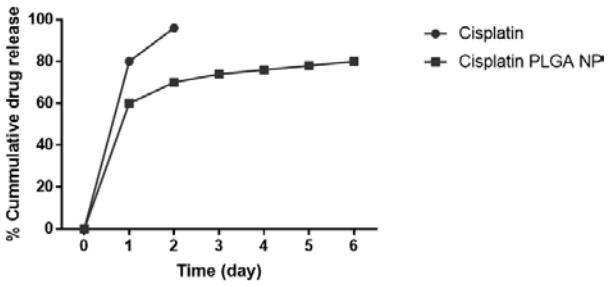

Figure 13. *In-vitro* drug release study of pure cisplatin and cisplatin PLGA NPs in PBS (pH 7.4).

4. Conclusion

The cisplatin-loaded PLGA nanoparticles were made using the double emulsion solvent evaporation process. A second-order model was fitted to the response data of the cisplatin PLGA nanoparticles using the central composite rotatable design–responsive surface approach. Most of the nanoparticles' experimental values were in line with their projected values. The obtained nanoparticles were found to be spherical in shape confirmed by scanning electron microscopy. Nanoparticle-mediated drug release followed a biphasic pattern, with early burst releases followed by a sustained release. *In vitro* drug release trials using nanoparticles showed a long-term effect. According to these findings, the nanoparticles developed in this work might be used therapeutically as a carrier with an initial dosage and a sustained plasma level *in vivo*.

Conflict of interest

The authors declare that they have no conflict of interest.

References

1. Attia MF, Anton N, Wallyn J, *et al.* An overview of active and passive targeting strategies to improve the nanocarriers efficiency to tumor sites. Journal of Pharmacy and Pharmacology 2019; 71(8): 1185–1198.
2. Danaei M, Dehghankhold M, Ataei S, *et al.* Impact of particle size and polydispersity index on the clinical applications of lipidic nanocarrier systems. Pharmaceutics 2018; 10(2): 57.
3. Shehata T, Kimura T, Higaki K, *et al.* In-vivo disposition characteristics of PEG niosome and its interaction with serum proteins. International Journal of Pharmaceutics 2016; 512(1): 322–328.
4. Kreuter J, Hekmatara T, Dreis S, *et al.* Covalent attachment of apolipoprotein AI and apolipoprotein B-100 to albumin nanoparticles enables drug transport into the brain. Journal of Controlled Release 2007; 118(1): 54–58.
5. Jiang W, Kim BYS, Rutka JT, *et al.* Advances and challenges of nanotechnology-based drug delivery systems. Expert Opinion on Drug Delivery 2007; 4(6): 621–633.
6. Lövestam G, Rauscher H, Roebben G, *et al.* Considerations on a definition of nanomaterial for regulatory purposes. Joint Research Centre (JRC) Reference Reports. Luxembourg: Publications Office of the European Union; 2010. p. 00–41.
7. Zeng X, Tao W, Wang Z, *et al.* Docetaxel-loaded nanoparticles of dendritic amphiphilic block copolymer H40-PLA-b-TPGS for cancer treatment. Particle & Particle Systems Characterization 2015; 32(1): 112–122.
8. Venkatasubbu GD, Ramasamy S, Avadhani GS, *et al.* Surface modification and paclitaxel drug delivery of folic acid modified polyethylene glycol functionalized hydroxyapatite nanoparticles. Powder Technology 2013; 235: 437–442.
9. Yang S, Zhou L, Su Y, *et al.* One-pot photoreduction to prepare NIR-absorbing plasmonic gold nanoparticles tethered by amphiphilic polypeptide copolymer for synergistic photothermal-chemotherapy. Chinese Chemical Letters 2019; 30(1): 187–191.

10. Peng Y, Nie J, Cheng W, *et al.* A multifunctional nanoplatform for cancer chemo-photothermal synergistic therapy and overcoming multidrug resistance. Biomaterials Science 2018; 6(5): 1084–1098.
11. Reis CP, Neufeld RJ, Ribeiro AJ, *et al.* Nanoencapsulation I: Methods for preparation of drug-loaded polymeric nanoparticles. Nanomedicine: Nanotechnology, Biology and Medicine 2006; 2(1): 8–21.
12. Rao JP, Geckeler KE. Polymer nanoparticles: Preparation techniques and size-control parameters. Progress in Polymer Science 2011; 36(7): 887–913.
13. Pal SL, Jana U, Manna PK, *et al.* Nanoparticle: An overview of preparation and characterization. Journal of Applied Pharmaceutical Science 2011; 1(6): 228–234.
14. Vaughn DJ. Paclitaxel and carboplatin in bladder cancer: Recent developments. European Journal of Cancer 2000; 36: 7–12.
15. Yan X, Gemeinhart R A. Cisplatin delivery from poly (acrylic acid-co-methyl methacrylate) microparticles. Journal of Controlled Release 2005; 106(1–2): 198–208.
16. Cvitkovic E. Cumulative toxicities from cisplatin therapy and current cytoprotective measures. Cancer Treatment Reviews 1998; 24(4): 265–281.
17. Van Leeuwen BL, Kamps WA, Jansen HWB, *et al.* The effect of chemotherapy on the growing skeleton. Cancer Treatment Reviews 2000; 26(5): 363–376.
18. Gamal Eid A, Uddin N, Girgis S. Formulation and optimization of biodegradable insulin loaded nanoparticles. European Journal of Biotechnology and Bioscience 2019; 7(4): 10–21.
19. Zhang X, Liu J, Qiao H, *et al.* Formulation optimization of dihydroartemisinin nanostructured lipid carrier using response surface methodology. Powder Technology 2010; 197(1–2): 120–128.
20. Avgoustakis K, Beletsi A, Panagi Z, *et al.* PLGA–mPEG nanoparticles of cisplatin: in vitro nanoparticle degradation, in vitro drug release and in vivo drug residence in blood properties. Journal of Controlled Release 2002; 79(1–3): 123–135.
21. Agrahari V, Kabra V, Trivedi P. Development, optimization and characterization of nanoparticle drug delivery system of Cisplatin. 13th International Conference on Biomedical Engineering; 2008 Dec 3–6; Singapore. Heidelberg: Springer; 2009. p. 1325–1328.
22. Zhang X, Liu J, Qiao H, *et al.* Formulation optimization of dihydroartemisinin nanostructured lipid carrier using response surface methodology. Powder Technology 2010; 197(1–2): 120–128.
23. Nair KGS, Velmurugan R, Sukumaran SK. Formulation and optimization of ansamycin-loaded polymeric nanoparticles using response surface methodology for bacterial meningitis. BioNanoScience 2020; 10(1): 279–291.
24. Mehnert W, Mäder K. Solid lipid nanoparticles: production, characterization and applications. Advanced Drug Delivery Reviews 2012; 64: 83–101.
25. Tadros TF, Vincent B. Influence of temperature and electrolytes on the adsorption of poly (ethylene oxide)-poly (propylene oxide) block copolymer on polystyrene latex and on the stability of the polymer-coated particles. The Journal of Physical Chemistry 1980; 84(12): 1575-1580.
26. Krishnamachari Y, Madan P, Lin S. Development of pH- and time-dependent oral microparticles to optimize budesonide delivery to ileum and colon. International Journal of Pharmaceutics 2007; 338(1–2): 238–247.